

# Black Holes and Black Hole Entropy

Talk by Laura Sagunski,  
Workshop Seminar on “Holography”,  
Summer Term 2015

April 21, 2015

---

## Contents

<b>1</b>	<b>Introduction</b>	<b>1</b>
<b>2</b>	<b>Geometry of Black Holes</b>	<b>3</b>
<b>3</b>	<b>Black Holes and Quantum Mechanics</b>	<b>6</b>
<b>4</b>	<b>Black Hole Thermodynamics</b>	<b>9</b>

---

## 1 Introduction

The aim of this talk is to give an overview of the physical properties of black holes, including their geometric description, and to derive the black hole thermodynamics from quantum mechanical principles.

If not marked otherwise, I will refer to the results presented in the textbook [1] and the reviews [2–4]. We will start with the general definition of a black hole.

### 1.1 Classification of black holes

In general, a black hole is a mathematically defined region of space with a sufficiently compact mass  $M$  which exhibits such a strong gravitational force that no particle or electromagnetic radiation can escape from it [5, 6].

Black holes are commonly classified according to their mass  $M$ . While one distinguishes between *supermassive*, *intermediate-mass* and *stellar black holes* in Astrophysics, a (hypothetical) class of *primordial black holes* of cosmological origin exists (confer Tab. 1.0).

There is a general consensus that *supermassive black holes*, with masses of  $10^5 \dots 10^{10} M_\odot$  in terms of the mass of the Sun  $M_\odot$ , are found in the center of most galaxies, including the Milky Way [7].

Classification	$M$	$r_s$
Supermassive	$10^5 \dots 10^{10} M_\odot$	$0.01 \dots 400 \text{ AU}$
Intermediate-mass	$10^3 M_\odot$	$10^3 \text{ km} \simeq R_E$
Stellar	$10 M_\odot$	$30 \text{ km}$
Primordial	$\lesssim M_\zeta$	$\lesssim 0.1 \text{ mm}$

Table 1.0: Classification of black holes by their mass  $M$  and/or the corresponding Schwarzschild radius  $r_s \propto M$ . The reference masses are the mass of the Sun,  $M_\odot \simeq 10^{30} \text{ kg}$ , and the Moon,  $M_\zeta \simeq 10^{23} \text{ kg}$ , whereas length specifications are given in terms of the distance between Earth and Sun,  $1 \text{ AU} \simeq 10^8 \text{ km}$ , and the Earth radius  $R_E$ .

*Stellar black holes* are formed by the gravitational collapse of a massive star at the end of its lifetime [8] and have typical masses of the order of  $10 M_\odot$ . They can grow by accretion of matter and by merging with other black holes.

Currently, the existence of *intermediate-mass black holes* [9] with masses around  $10^3 M_\odot$  is only based on indirect detection methods. However, they are believed to form due to mergings or collisions of stellar black holes or other compact objects.

(Hypothetical) *primordial black holes* are supposed not to have formed by gravitational collapse of a star, but due to the extreme density of matter in the Early Universe. One estimates their masses to be less or equal to the mass of the Moon  $M_\zeta$ . Furthermore, they have been proposed as a candidate for dark matter [10].

## 1.2 Schwarzschild radius

Instead of using the mass  $M$  as classification parameter, we can also classify black holes in terms of the so-called Schwarzschild radius  $r_s \propto M$ . In order to illustrate the physical meaning of the Schwarzschild radius, we use classical Newtonian mechanics as starting point.

Let us consider a particle with mass  $m$  in the gravitational field of a spherically symmetric object with mass  $M$ . For escaping from this object, the kinetic energy of the particle has to be bigger than its potential energy in the gravitational field. This condition allows us to determine the necessary escape velocity of the particle,

$$\frac{1}{2} m v_{\text{esc}}^2 > \frac{GMm}{r} \quad \Rightarrow \quad v_{\text{esc}} > \sqrt{\frac{2GM}{r}}, \quad (1.1)$$

which is independent of its mass  $m$ . Here,  $G$  denotes the Newtonian gravitational constant and  $r$  corresponds to the distance between the particle and the object.

By definition black holes prevent any particle to escape from their gravitational force. In other words, this requires the necessary escape velocity  $v_{\text{esc}}$  of the particle to be bigger than the speed of light  $c \equiv 1$ . The escape velocity exceeds the speed of light,

$$v_{\text{esc}} > 1 \quad \Leftrightarrow \quad r < r_s = 2GM, \quad (1.2)$$

if the particle approaches closer than the *Schwarzschild radius*  $r_s$  of the black hole. The boundary at  $r = r_s$  is referred to as *horizon* of the black hole.

While the Schwarzschild radii  $r_s$  of supermassive black holes lie in the range of  $0.01 \dots 400$  AU, they are of order 30 km for stellar black holes and even less than 0.1 mm for primordial black holes (see Tab. 1.0).

## 2 Geometry of Black Holes

Before studying the quantum theory of black holes, we review the geometry of classical black holes in two different coordinate systems, namely in Schwarzschild coordinates and in so-called near-horizon coordinates.

### 2.1 Schwarzschild coordinates

We begin with the simplest spherically symmetric, static, uncharged black hole described by the  $(3 + 1)$  dimensional Schwarzschild metric,

$$\begin{aligned} ds^2 &= g_{\mu\nu} dx^\mu dx^\nu \\ &= \left(1 - \frac{r_s}{r}\right) dt^2 - \left(1 - \frac{r_s}{r}\right)^{-1} dr^2 - r^2 d\Omega^2, \end{aligned} \tag{2.1}$$

where  $d\Omega^2 = d\theta^2 + \sin^2\theta d\varphi^2$ . The coordinate  $t$ , corresponding to the time recorded by a standard clock at spatial infinity, is named Schwarzschild time, whereas  $r$  denotes the Schwarzschild radial coordinate and is defined so that the area of the 2-sphere at  $r$  is  $4\pi r^2$ . Moreover, the angles  $\theta$  and  $\varphi$  constitute the usual polar and azimuthal angles.

The horizon of the black hole, which is defined as the place where  $g_{tt} = 0$ , arises at the Schwarzschild radius  $r = r_s$  (confer Sec. 1.2). At the horizon  $g_{rr}$  becomes singular. However, as we will see in the following, the horizon does not constitute a usual local mathematical singularity of the metric (such as  $r = 0$ ), but is *globally* special. In particular, no local invariant properties of the geometry become singular at  $r = r_s$ .

For example, a radially infalling observer with a small laboratory would pass the horizon smoothly and would record nothing unusual. For a distant observer, however, the crossing of the horizon does not occur at any finite Schwarzschild time since  $r \rightarrow r_s$  in (2.1) implies  $t \rightarrow \infty$ . The other way round, a signal originating at (or behind) the horizon cannot reach the distant observer until an infinite Schwarzschild time has passed. Thus, to a distant observer the horizon represents the boundary of the world since no information can be transmitted from there.

Let us now investigate further the region near the horizon by introducing an appropriate coordinate system.

### 2.2 Near-horizon coordinates (Rindler space)

We can study the near-horizon region by replacing the Schwarzschild radial coordinate  $r$  by a coordinate  $\rho$  which measures the proper distance from the horizon,

$$\rho = \int_{r_s}^r dr' \sqrt{g_{rr}(r')} = \int_{r_s}^r dr' \left(1 - \frac{r_s}{r'}\right)^{-\frac{1}{2}} \simeq 2\sqrt{r_s(r - r_s)}, \tag{2.2}$$

where the last approximation is true near the horizon,  $r \simeq r_s$ . Using  $d\rho^2 = [1 - (r_s/r)]^{-1} dr^2$  allows us to rewrite the Schwarzschild metric (2.1) in terms of the coordinates  $t$  and  $\rho$ ,

$$ds^2 = \rho^2 \left( \frac{dt}{2r_s} \right)^2 - d\rho^2 - r^2(\rho) d\Omega^2, \quad (2.3)$$

In addition, we introduce a dimensionless time  $\omega$ , defined as

$$\omega = \frac{t}{2r_s} = \frac{t}{4MG}, \quad (2.4)$$

and restrict our considerations to a small angular region of the horizon arbitrarily centered around  $\theta = 0$ . Then, we can replace the angular coordinates by Cartesian coordinates

$$X = r_s \sin \theta \cos \varphi, \quad Y = r_s \sin \theta \sin \varphi \quad (2.5)$$

where  $\sin \theta \simeq \theta$ . With  $r(\rho) \simeq r_s$  and  $d\Omega^2 \simeq d\theta^2 + \theta^2 d\varphi^2$  the metric (2.3) then takes the form

$$ds^2 = \rho^2 d\omega^2 - d\rho^2 - dX^2 - dY^2. \quad (2.6)$$

If we finally transform  $\rho$  and  $\omega$  to the coordinates

$$T = \rho \sinh \omega, \quad Z = \rho \cosh \omega, \quad (2.7)$$

we end up with the familiar Minkowski metric,

$$ds^2 = dT^2 - dZ^2 - dX^2 - dY^2. \quad (2.8)$$

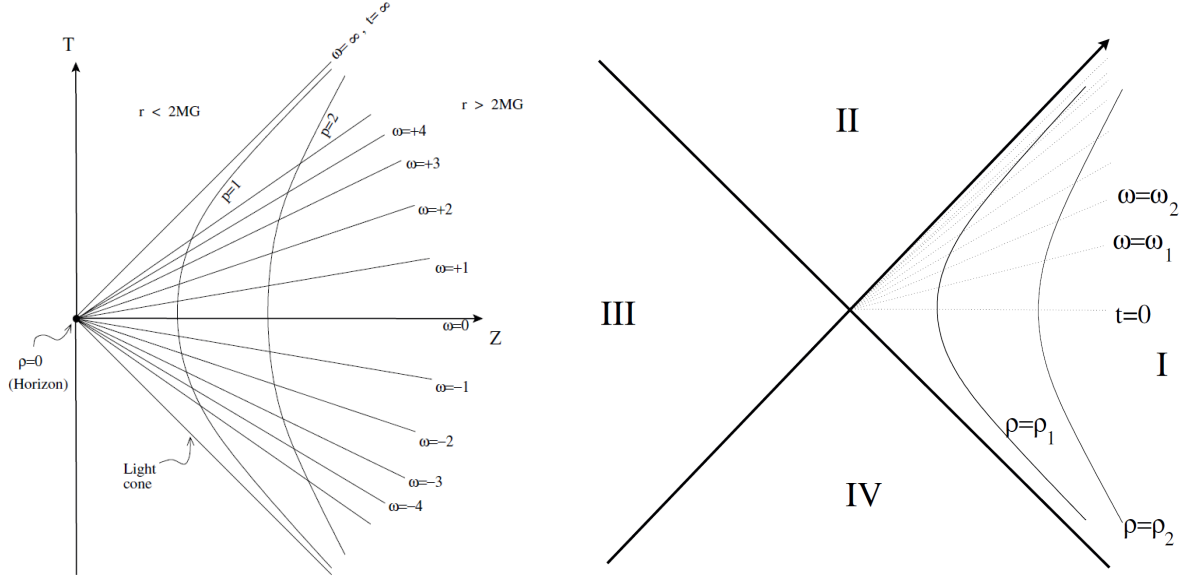
Note that this relation is only valid near the horizon, where  $r \simeq r_s$  or equivalently  $\rho \simeq 0$  (confer (2.2)), and only for a small angular region. However, it is now evident that  $\rho$  and  $\omega$  are the radial and hyperbolic angle coordinates of an ordinary Minkowski space. Consequently, the near-horizon geometry is just Minkowski spacetime described in hyperbolic polar coordinates. Thus, the horizon, for a large black hole, is locally almost indistinguishable from flat space-time.

In Fig. 2.1 the relation between the Minkowski coordinates  $T$  and  $Z$  and the near-horizon coordinates  $\rho$  and  $\omega$  is shown. As in particular illustrated in Fig. 2.1a, the black hole horizon, constituting the boundary  $r = r_s$ , is located at the origin where  $\rho = 0$  and hence  $T = Z = 0$  (see (2.7)). Fig. 2.1b shows that the horizon divides the entire Minkowski space into four quadrants labeled I, II, III and IV. Only one of those Minkowski regions, namely Region I, lies outside the horizon. This region is called *Rindler space*. According to that, one denotes the dimensionless time  $\omega$  in (2.4) as Rindler time.

A useful way to illustrate the causal structure of spacetimes are Penrose diagrams. The Penrose diagram of a black hole is explained in App. A.

### 3 Black Holes and Quantum Mechanics

So far, we have only discussed the behavior of classical particles near the black hole horizon. However, to investigate the thermodynamic characteristics of the black hole like for example its temperature and entropy, it is necessary to study the behavior of quantum fields in the near-horizon region, i.e. in Rindler space.



(a) Illustration of the black hole horizon, located at the origin  $\rho = 0$  or equivalently at  $T = Z = 0$  [1]. (b) Illustration of the Rindler space (Region I) being the Minkowski-space approximation outside the horizon [1].

Fig. 2.1: Relation between Minkowski coordinates  $T$  and  $Z$  and Rindler coordinates  $\rho$  and  $\omega$ .

Let us imagine two quantum fields located at different spatial points on *opposite* sides of the horizon. Although the correlation of those fields is not measurable by an observer outside the horizon, it has significance. When two subsystems (here the fields inside and outside of the horizon) become correlated, we say that they are *quantum entangled*. In consequence, none of them can be described in terms of a pure state. The appropriate description of an entangled subsystem is achieved by means of a density matrix.

### 3.1 Review of the density matrix and entropy

A quantum system consisting of two subsystems A and B, which have previously been in contact, but are no longer interacting, has a wave function

$$\Psi = \Psi(\alpha, \beta) , \quad (3.1)$$

where  $\alpha$  and  $\beta$  are appropriate commuting variables for the subsystems A and B. If we are interested in the subsystem A (or B equivalently), the density matrix

$$\rho_A(\alpha, \alpha') = \sum_{\beta} \Psi^*(\alpha, \beta) \Psi(\alpha', \beta) \quad (3.2)$$

provides a complete description of all measurements in A. In particular, the expectation value of an operator  $\mathbf{a}$  is computed in terms of the density matrix as  $\langle \mathbf{a} \rangle = \text{Tr}(\mathbf{a} \rho_A)$ . Density matrices have the properties that their total probability equals 1 ( $\text{Tr} \rho = 1$ ), that they are hermitian ( $\rho = \rho^\dagger$ ) and that all their eigenvalues are positive or zero ( $\rho_j \geq 0$ ). In the representation where  $\rho$  is diagonal, an eigenvalue  $\rho_j$  correspond to the probability that the systems is in the state  $|j\rangle$ . If only one eigenvalue  $\rho_j$  is non-zero, the density matrix is indistinguishable from a pure state and the respective wave function is an uncorrelated product of the form

$$\Psi = \Psi_A(\alpha) \Psi_B(\beta) . \quad (3.3)$$

A quantitative measure of the departure from a pure state and hence a measure of the degree of entanglement is provided by the *Von Neumann (entanglement) entropy*,

$$S_N = -\text{Tr}(\rho \log \rho) = -\sum_j \rho_j \log \rho_j. \quad (3.4)$$

Only for a pure state we have  $S_N = 0$  since then all eigenvalues except from one are zero and due to the trace condition the non-trivial eigenvalue just equals 1. Moreover, the Von Neumann entropy provides also a measure of the number of quantum states in the statistical ensemble.

The Von Neumann entropy should not be confused with the thermal entropy of the second law of thermodynamics. If a system with Hamiltonian  $H$  is in thermal equilibrium at a temperature  $T \equiv 1/\beta$ , it is described by a Maxwell-Boltzmann density matrix

$$\rho_{\text{MB}} = \frac{e^{-\beta H}}{\text{Tr}(e^{-\beta H})}. \quad (3.5)$$

In this case, the *thermal entropy* is given by

$$S = -\text{Tr}(\rho_{\text{MB}} \log \rho_{\text{MB}}). \quad (3.6)$$

### 3.2 The Unruh density matrix

An observer in Rindler space outside the horizon has no access to the quantum states behind the horizon. Consequently, all measurements of the observer have to be described in terms of a Rindler-space density matrix  $\rho_R$  which is obtained by tracing over the degrees of freedom behind the horizon.

To derive the form of the density matrix  $\rho_R$ , we first consider the flat Minkowski spacetime as seen by the observer in Rindler space. Fig. 2.1 shows that the Rindler time  $\omega = 0$  coincides with the half-surface in Minkowski space where  $T = 0$  and  $Z > 0$ . The other half of the surface where  $Z < 0$  lies behind the horizon and consequently has to be traced over.

Let us now consider a set of quantum fields  $\phi$ . In order to specify the field configuration at  $T = 0$ , we need to assign values to  $\phi$  both behind (inside) and outside the horizon,

$$\phi = \begin{cases} \phi_{\text{in}} & \text{for } Z < 0 \\ \phi_{\text{out}} & \text{for } Z > 0. \end{cases} \quad (3.7)$$

The non-trivial entanglement between the degrees of freedom of  $\phi_{\text{in}}$  and  $\phi_{\text{out}}$  cause the density matrix outside the horizon to be a mixed state. Hence, the wave function of the total system is a functional of  $\phi_{\text{in}}$  and  $\phi_{\text{out}}$  (confer (3.1)),

$$\Psi(\phi) = \Psi(\phi_{\text{in}}, \phi_{\text{out}}). \quad (3.8)$$

In order to determine  $\Psi$ , we assume that the field theory is described in terms of an action denoted by  $I$  (to avoid confusion with the entropy  $S$ ),

$$I = \int d^3X dT \mathcal{L}. \quad (3.9)$$

By transforming to imaginary time  $T = i\tau$  with  $\tau > 0$ , we obtain the Euclidean action  $I_E$ . This allows us to calculate  $\Psi$  by use of the standard Feynman path integral formula,

$$\Psi(\phi_{\text{in}}, \phi_{\text{out}}) = \int d\phi e^{-I_E}, \quad (3.10)$$

where the path integral is over all fields in the future half space  $\tau > 0$  with boundary condition  $\phi = \phi_{\text{out}} = \phi_{\text{in}}$  at  $\tau = 0$ . The trick to compute (3.10) is now to divide the half plane  $\tau > 0$  in infinitesimal angular wedges and then to evaluate the path integral in terms of a generator of angular rotations (for more details see [11]). From the resulting expression,

$$\Psi(\phi_{\text{in}}, \phi_{\text{out}}) = \langle \phi_{\text{in}} | e^{-\pi H_R} | \phi_{\text{out}} \rangle, \quad (3.11)$$

we see that  $\Psi$  arises as a transition matrix element between the states  $\phi_{\text{out}}$  and  $\phi_{\text{in}}$ . Moreover, it turns out that the angular generator is just the Rindler-space Hamiltonian  $H_R$ . By definition it is conjugate to the dimensionless Rindler time  $\omega$  and hence also dimensionless,

$$[H_R, \omega] = i. \quad (3.12)$$

Inserting  $w = t/(4MG)$  in the previous equation and using the fact that usual Minkowski-space Hamiltonian  $H$ , which represents the energy of the black hole, is conjugate to the Schwarzschild time  $t$ , i.e.  $[H, t] = i$ , we can derive the relation between the Hamiltonian in Minkowski and Rindler space,

$$H = \frac{1}{4MG} H_R. \quad (3.13)$$

Now we are ready to compute the Rindler-space density matrix  $\rho_R$  from the definition (3.2),

$$\rho_R(\phi_{\text{out}}, \phi'_{\text{out}}) = \int d\phi_{\text{in}} \Psi^*(\phi_{\text{in}}, \phi'_{\text{out}}) \Psi(\phi_{\text{in}}, \phi_{\text{out}}). \quad (3.14)$$

Using the result (3.11) and the completeness of the states  $|\phi_{\text{in}}\rangle$  yields

$$\begin{aligned} \rho_R(\phi_{\text{out}}, \phi'_{\text{out}}) &= \int d\phi_{\text{in}} \langle \phi_{\text{out}} | e^{-\pi H_R} | \phi_{\text{in}} \rangle \langle \phi_{\text{in}} | e^{-\pi H_R} | \phi'_{\text{out}} \rangle \\ &= \langle \phi'_{\text{out}} | e^{-2\pi H_R} | \phi_{\text{out}} \rangle. \end{aligned} \quad (3.15)$$

More concisely, the density matrix is given by the operator

$$\rho_R = e^{-2\pi H_R} = e^{-\beta_R H_R} \quad (3.16)$$

with

$$\boxed{T_R = \frac{1}{\beta_R} = \frac{1}{2\pi}}. \quad (3.17)$$

Thus, we conclude that the observer in Rindler space outside the horizon sees the vacuum as a *thermal ensemble* with a density matrix of the Maxwell-Boltzmann type (3.5) and a temperature  $T_R$ . This remarkable result was discovered by William Unruh in 1976 [11].

## 4 Black Hole Thermodynamics

### 4.1 Hawking temperature

Like the Rindler time  $\omega$  and the corresponding Hamiltonian  $H_R$ , the temperature  $T_R$  is dimensionless. To convert it into a proper temperature with dimensions of energy, we consider the proper time in Rindler space. It can be read off from the metric (2.6),  $ds = \rho d\omega$ . Consequently, an observer located at a distance  $\rho$  from the horizon converts dimensionless quantities by using the conversion factor  $1/\rho$ . According to that, the proper temperature at the distance  $\rho$  reads

$$T(\rho) = \frac{1}{\rho} T_R = \frac{1}{2\pi\rho}. \quad (4.1)$$

with  $T_R$  given in (3.17). Hence, an observer near the horizon of the black hole detects a temperature which varies as the inverse distance from the horizon. When approaching the horizon,  $\rho \rightarrow 0$ , the temperature increases towards infinity,  $T(\rho) \rightarrow \infty$ .

Let us now determine the temperature measured by a distant observer asymptotically far from the black hole. Instead of the near-horizon Rindler time  $\omega$ , the appropriate time variable for such an observer is the Schwarzschild time  $t = 4MG\omega$ . Hence, a quantum field with Rindler frequency  $\nu_R$  is seen by the distant Schwarzschild observer to have a red-shifted frequency

$$v = \frac{1}{4MG} \nu_R. \quad (4.2)$$

This implies that the Rindler temperature  $T_R$  is recognized to be red-shifted, too. Thus, the temperature of the black hole measured by a *distant* observer equals

$$\boxed{T_H = \frac{1}{4MG} T_R = \frac{1}{8\pi MG}}. \quad (4.3)$$

The temperature  $T_H$  represents the true thermodynamic temperature of the black hole. It was first calculated by Stephen Hawking in 1975 [12] and is therefore named *Hawking temperature*.

From the fact that the region near the horizon has a non-vanishing temperature, one expects thermal effects, such as evaporation, to occur. Indeed, the black hole has a kind of thermal atmosphere consisting of thermally excited quantum states [13]. Some of these quanta have sufficient energy to escape the gravitational potential of the black hole and are emitted in form of ordinary black body radiation. This thermal radiation of the black hole is the so-called *Hawking radiation*.

### 4.2 Bekenstein-Hawking entropy

In the last section, we derived that a black hole appears to a distant observer as a body with Hawking temperature  $T_H$  and energy  $E = M$  equivalent to its mass. As a consequence of thermodynamics, it follows that the black hole must also have an entropy  $S$ . The thermodynamic relation between energy and temperature, i.e. the *first law of thermodynamics*,

$$dE = T dS, \quad (4.4)$$

allows us to compute the entropy  $S$  of the black hole. Replacing the energy  $E$  by the black hole mass  $M$  and inserting for  $T$  the Hawking temperature  $T_H$ , given in (4.3), yields

$$dM = \frac{1}{8\pi MG} dS. \quad (4.5)$$



Therefore, the resulting expression for the entropy of the black hole reads

$$S = 4\pi M^2 G. \quad (4.6)$$

Since the Schwarzschild radius is defined as  $r_s = 2MG$ , the area of the black hole horizon equals

$$A = 4\pi r_s^2 = 16\pi M^2 G^2 \quad (4.7)$$

so that we can rewrite the entropy (4.6) in the following form,

$$\boxed{S_{\text{BH}} = \frac{A}{4G}}. \quad (4.8)$$

which is known as *Bekenstein-Hawking entropy* [14]. Note that the black hole entropy is not proportional to the volume, as one would expect, but to the area of the horizon. We can understand this since we have seen that the temperature gets large in the vicinity of the horizon. Thus, the entropy is mainly stored near the horizon and therefore grows like the area.

The Bekenstein-Hawking entropy  $S_{\text{BH}}$  has to be understood as both entanglement and thermal entropy in the special case of the Rindler-space density matrix. Including the quantum effects behind the horizon through integration over the fields  $\phi_{\text{in}}$  in (3.14) led to the surprising physical effect of producing a thermal density matrix (confer (3.16)). This allowed us to reduce the computation of the black hole entropy to ordinary thermodynamic methods.

Note that equation (4.8) is far more general than one would expect from the derivation given here. It holds for any kind of black hole no matter if rotating, charged or in arbitrary dimensions. In the general  $(d+1)$  dimensional case, the concept of a two dimensional area only needs to be replaced by the  $(d+1)$  dimensional measure of the horizon.

### 4.3 Maximum entropy

As an example for applying the Bekenstein-Hawking entropy (4.8), let us now consider the formation of a black hole. Imagine a spherically symmetric shell of matter with a certain entropy which collapses into a black hole. After the formation of the black hole, the total entropy of the system is given by the Bekenstein-Hawking formula,  $S_{\text{BH}} = A/(4G)$ .

According to the *second law of thermodynamics*, the entropy in a thermodynamic process does always increase,

$$dS \geq 0. \quad (4.9)$$

Consequently, the original entropy of the matter shell had to be less or equal than the entropy of the black hole,

$$S_{\text{max}} \leq \frac{A}{4G}. \quad (4.10)$$

This bound on the maximum entropy has to hold for *any* system and is called the *holographic limit*.

However, it turns out that quantum field theory does not describe the degrees of freedom and hence the entropy of a gravitational system consistently. Indeed, there are vastly fewer degrees of freedom in string theory. The *holographic principle* is about counting the quantum states of a system and hence determining its entropy correctly. We will hear more about the holographic principle in the next talk.

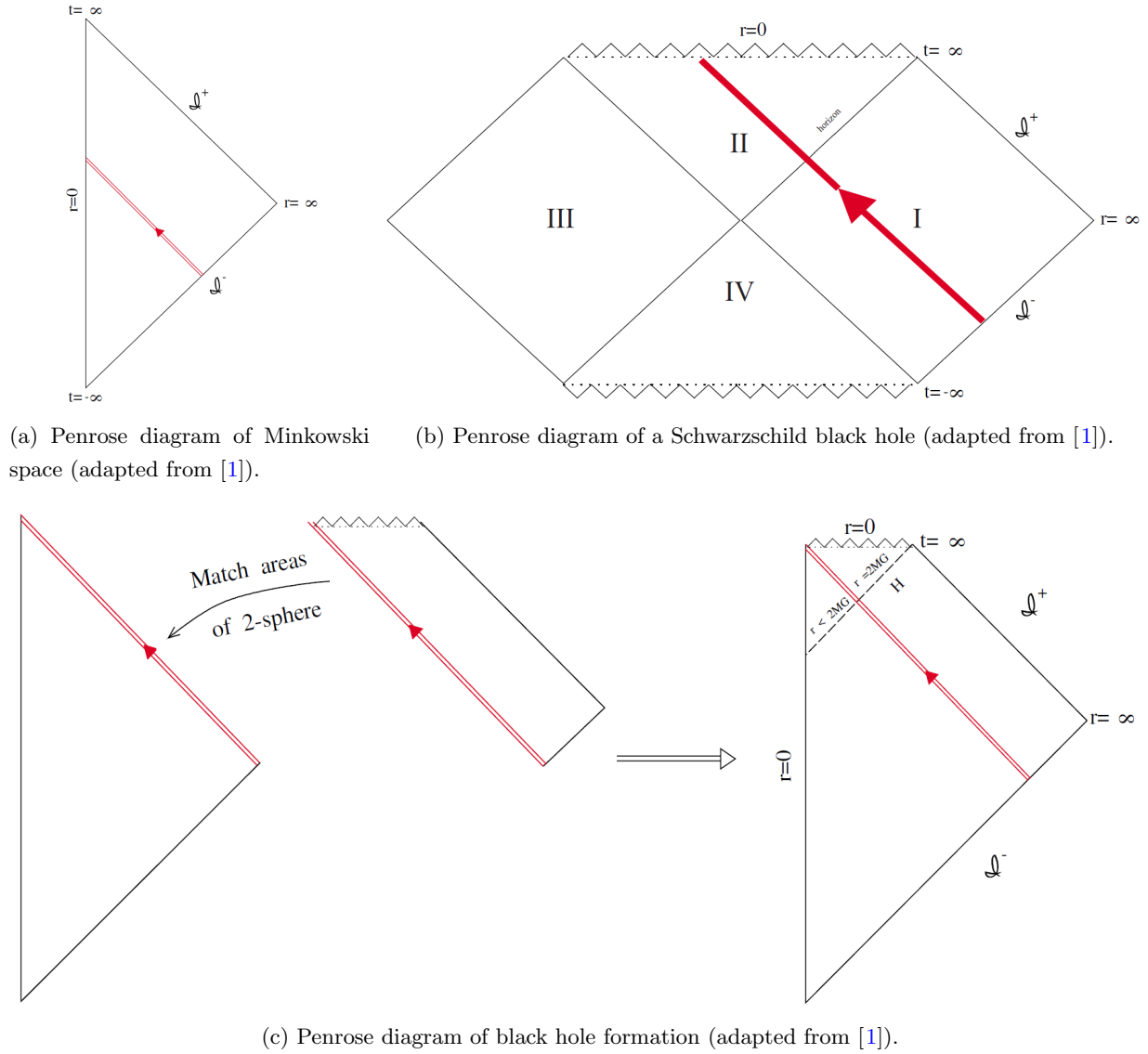


Fig. 1.2: Penrose diagrams describing the full evolution of a black hole.

## A Penrose diagram of a black hole

### A.1 Review of Penrose diagrams

Penrose diagrams illustrate the causal structure of spacetimes very intuitively. They represent the geometry of a two-dimensional surface of fixed angular coordinates in spacetime. Furthermore, they “compactify” the geometry so that it can be drawn in total on a finite plane. The coordinates mapping the entire geometry to the finite plane should be chosen such that radial light rays correspond to lines oriented at  $45^\circ$  to the vertical axis. As an example, the Penrose diagram for a flat Minkowski space, parametrized by spherical coordinates with time  $t$  and radial distance  $r$ , is shown in Fig. 1.2a. The vertical axis represents the spatial origin  $r = 0$ . Apart from that, there are several infinities such as a space-like infinity ( $r = \infty$ ) and future and past time-like infinities ( $t = \pm\infty$ ). Light rays enter from past light-like infinity  $\mathcal{I}^-$  and exit at future light-like infinity  $\mathcal{I}^+$ .

## A.2 Penrose diagram of black hole formation

The Penrose diagram of a Schwarzschild black hole is depicted in Fig. 1.2b. While Region I, the Rindler space, corresponds to the outside of the black hole and possesses space-like, time-like as well as past and future light-like infinities, Region II is identified as being behind the horizon. Any future-directed light ray which begins in Region II will reach  $r = 0$ .

A real black hole forms by gravitational collapse. In the remote past before the formation of the black hole, the geometry just corresponds to the lower portion of Minkowski space in Fig. 1.2a, whereas at late times, when the black hole has formed, it is described by the Schwarzschild geometry. Thus, we obtain the Penrose diagram for the full evolution of the black hole by “gluing” the lower left and the upper right region of Fig. 1.2a and Fig. 1.2b together. Note that thereby the continuity of the variable  $r$  is respected since it varies monotonically from  $r = \infty$  at  $\mathcal{I}^-$  to  $r = 0$  in both cases. The resulting Penrose diagram for the black hole formation is depicted in Fig. 1.2c.

## References

- [1] L. Susskind and J. Lindesay, *An Introduction to Black Holes, Information and the String Theory Revolution: The Holographic Universe*. World Scientific, 2005.
- [2] D. Bigatti and L. Susskind, *TASI lectures on the holographic principle*, [hep-th/0002044](#).
- [3] R. Bousso, *The Holographic principle*, *Rev.Mod.Phys.* **74** (2002) 825–874, [[hep-th/0203101](#)].
- [4] J. A. Harvey and A. Strominger, *Quantum aspects of black holes*, [hep-th/9209055](#).
- [5] R. M. Wald, *The thermodynamics of black holes*, *Living Rev.Rel.* **4** (2001) 6, [[gr-qc/9912119](#)].
- [6] R. M. Wald, *Gravitational collapse and cosmic censorship*, [gr-qc/9710068](#).
- [7] R. Schodel, T. Ott, R. Genzel, R. Hofmann, M. Lehnert, et al., *Closest star seen orbiting the supermassive black hole at the centre of the Milky Way*, *Nature* (2002) [[astro-ph/0210426](#)].
- [8] A. Celotti, J. C. Miller, and D. W. Sciama, *Astrophysical evidence for the existence of black holes: Topical review*, *Class.Quant.Grav.* **16** (1999) A3, [[astro-ph/9912186](#)].
- [9] K. Gebhardt, R. M. Rich, and L. C. Ho, *An Intermediate-mass black hole in the globular cluster G1: Improved significance from new Keck and Hubble Space Telescope observations*, *Astrophys.J.* **634** (2005) 1093–1102, [[astro-ph/0508251](#)].
- [10] M. Kesden and S. Hanasoge, *Transient solar oscillations driven by primordial black holes*, *Phys.Rev.Lett.* **107** (2011) 111101, [[arXiv:1106.0011](#)].
- [11] W. Unruh, *Notes on black hole evaporation*, *Phys.Rev.* **D14** (1976) 870.

- [12] S. Hawking, *Particle Creation by Black Holes*, *Commun.Math.Phys.* **43** (1975) 199–220.
- [13] K. Thorne, R. Price, and D. MacDonald, *Black Holes: The Membrane Paradigm*. Silliman Memorial Lectures. Yale University Press, 1986.
- [14] J. Bekenstein, *Black holes and the second law*, *Lett.Nuovo Cim.* **4** (1972) 737–740.